

# High-efficiency laser-irradiation spheroidizing of NiCo<sub>2</sub>O<sub>4</sub> nanomaterials\*

LIU Pei-sheng (刘培生)<sup>1\*\*,</sup> WANG Hao (王浩)<sup>1,2,3,</sup> ZENG Hai-bo (曾海波)<sup>3,</sup> FAN Guang-ming (范广明)<sup>1,</sup> and LIU Ya-hong (刘亚鸿)<sup>1</sup>

1. Key Laboratory of ASIC Design of Jiangsu Province, College of Electronics and Information, Nantong University, Nantong 226019, China

2. College of Science, Nantong University, Nantong 226019, China

3. Jiangsu Key Laboratory of Advanced Micro & Nano Materials and Technology, Institute of Optoelectronics & Nanomaterials, College of Material Science and Engineering, Nanjing University of Science and Technology, Nanjing 210094, China

(Received 24 September 2016)

©Tianjin University of Technology and Springer-Verlag Berlin Heidelberg 2016

We realized the desired spheroidizing of NiCo<sub>2</sub>O<sub>4</sub> nanomaterials by laser irradiating NiCo<sub>2</sub>O<sub>4</sub> suspensions with different concentrations. The results reveal that the as-prepared samples are desired spheres with the maximal average size of 568 nm and the superior dispersity, which were obtained at the energy density of 0.30 J·pulse<sup>-1</sup>·cm<sup>-2</sup> and NiCo<sub>2</sub>O<sub>4</sub> suspension concentration of 0.2 mg·mL<sup>-1</sup>. However, the phase segregation, which was induced by large amounts of solid redox of Co<sup>3+</sup>/Co<sup>2+</sup> and Ni<sup>3+</sup>/Ni<sup>2+</sup>, also appears in the laser-irradiation process.

**Document code:** A **Article ID:** 1673-1905(2016)06-0401-4

**DOI** 10.1007/s11801-016-6205-0

As advanced functional nanomaterials, multi-metal oxides (e.g., NiCo<sub>2</sub>O<sub>4</sub>, ZnCo<sub>2</sub>O<sub>4</sub>, CuCo<sub>2</sub>O<sub>4</sub>, MnCo<sub>2</sub>O<sub>4</sub>) have been extensively applied in the energy and environment fields, because of their superior performances<sup>[1-3]</sup>. Recently, there are many researchers focusing on the synthesis, structure and properties of the spinel NiCo<sub>2</sub>O<sub>4</sub> oxide. As binary-metal semiconductor oxide, NiCo<sub>2</sub>O<sub>4</sub> possesses some unique physical-chemical performances, such as narrow direct bandgap of 2.1 eV, high conductivity and electrochemical activity<sup>[4,5]</sup>. It is generally assumed that there exist mixed valences cobalt ions (Co<sup>3+</sup>/Co<sup>2+</sup>) and nickel ions (Ni<sup>3+</sup>/Ni<sup>2+</sup>) in the spinel structure NiCo<sub>2</sub>O<sub>4</sub>. Among these, Ni atoms possess the octahedral sites in the spinel structure, and Co atoms distribute between the octahedral and tetrahedral sites. Therefore, it presents large amounts of solid redox of Co<sup>3+</sup>/Co<sup>2+</sup> and Ni<sup>3+</sup>/Ni<sup>2+</sup>, with apparent electro-catalytic activity<sup>[6,7]</sup>.

As we know, morphology and structure of nanomaterial can influence its electronic and band structures, further the optical, electronic, magnetic properties, etc. For NiCo<sub>2</sub>O<sub>4</sub> nanomaterial, many fabricated methods have been reported, including hydrothermal method and microwave-assisted method<sup>[8-10]</sup>. Wang<sup>[7]</sup> has achieved the control-synthesis of different morphology NiCo<sub>2</sub>O<sub>4</sub>

nanostructures by the simple hydrothermal method, without template or catalyst. It is found that the control-synthesis of NiCo<sub>2</sub>O<sub>4</sub> nanostructure has a urea-dependence, and can be applied to the electrochemical cell successfully. In our group, Li<sup>[11]</sup> has synthesized the double-shell NiCo<sub>2</sub>O<sub>4</sub> nanostructure with large surface area and high electrical conductivity, realizing the high specific capacitance up to 718 F·g<sup>-1</sup>.

In this paper, we achieve the spheroidizing of NiCo<sub>2</sub>O<sub>4</sub> nanomaterials by laser irradiating NiCo<sub>2</sub>O<sub>4</sub> suspensions with different parameters. The results indicate that the spheroidized NiCo<sub>2</sub>O<sub>4</sub> possesses larger specific surface area, and its applications can be extended to catalysis and electrochemical fields.

The representative experimental steps are as follows. Firstly, 2.5 mmol Ni(NO<sub>3</sub>)<sub>2</sub>·6H<sub>2</sub>O, 5.0 mmol Co(NO<sub>3</sub>)<sub>2</sub>·6H<sub>2</sub>O, 5.0 mmol hexamethylenetetramine and 50 mL deionized water were added into the 100 mL beaker respectively, with magnetic stirring for 30 min to mix them uniformly. Next, the mixed solution was equivalently enclosed into two high temperature reactors and placed into the oven, heating at 160 °C for 6 h. Finally, the as-prepared samples were located in the high temperature tube furnace, roasting for 2 h at 300 °C with the heating rate of 1 °C/min, and subsequently NiCo<sub>2</sub>O<sub>4</sub> nanomaterials can

\* This work has been supported by the National Key Basic Research Program of China (No.2014CB931702), the National Natural Science Foundation of China (Nos.51572128 and 11502116), the National Natural Science Foundation of China and the Research Grants Council (No.5151101197), and the Priority Academic Program Development of Jiangsu Higher Education Institutions.

\*\* E-mail: pslu@issp.ac.cn

be obtained. The NiCo<sub>2</sub>O<sub>4</sub> nanomaterials with different quantities were dispersed into the 10 mL deionized water with ultrasonic dispersion for 30 min, respectively. Next, NiCo<sub>2</sub>O<sub>4</sub> suspensions with different concentrations (from 0.1 mg·mL<sup>-1</sup> to 0.5 mg·mL<sup>-1</sup>) were irradiated by 532 nm Nd:YAG laser for 5—30 min at the energy density from 0.05 J·pulse<sup>-1</sup>·cm<sup>-2</sup> to 0.4 J·pulse<sup>-1</sup>·cm<sup>-2</sup>. Subsequently, the brown colloidal solutions will be obtained.

The X-ray diffraction (XRD) patterns were recorded on a multipurpose XRD system D8 Advance from Bruker with a Cu K $\alpha$  radiation ( $\lambda=0.154\ 06\ \text{nm}$ ). For scanning electron microscopic (SEM) examination, the colloidal solutions were dropped onto the silicon flake and evaporated in air at room temperature. SEM observations were conducted on an FEI Quanta 250FEG. The optical absorption spectra of the colloidal solution were recorded by a Cary 5E UV-vis-IR spectrometer.

Fig.1(a) indicates clearly that the as-prepared NiCo<sub>2</sub>O<sub>4</sub> nanomaterial is the spinel structure (JCPDS No.20-0781), presenting no impurity diffraction peaks, which means the high purity. Six diffraction peaks correspond to NiCo<sub>2</sub>O<sub>4</sub> (220), (311), (222), (400), (511) and (440) planes, respectively. Fig.1(b) shows its UV-vis absorption spectrum, and there is obvious band edge absorption around 300 nm and 560 nm, which is consistent with the previous report<sup>[12]</sup>. The as-prepared NiCo<sub>2</sub>O<sub>4</sub> nanomaterial is irregular flower-like or sheet, including lots of cross-coupling nanorods, as shown in Fig.2. Due to only the raw materials in this case, further characterization of the as-prepared NiCo<sub>2</sub>O<sub>4</sub> nanomaterials can refer to our previous report<sup>[11]</sup>.

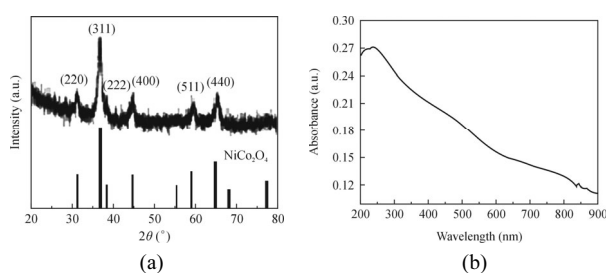


**Fig.1 (a) XRD pattern and (b) UV-vis spectrum of raw NiCo<sub>2</sub>O<sub>4</sub> nanomaterials**

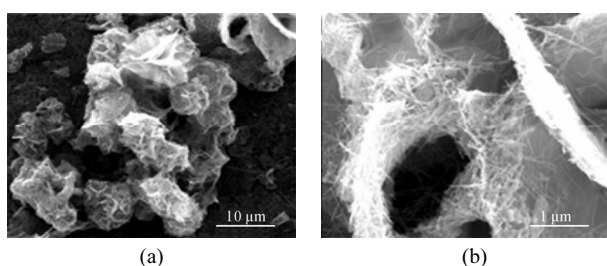


**Fig.2 SEM images of raw NiCo<sub>2</sub>O<sub>4</sub> nanomaterials with different scales**

As we all know, different synthesis methods have obvious impacts on the structure, morphology and performance of the nanomaterials. Here, we have achieved

the spheroidizing of NiCo<sub>2</sub>O<sub>4</sub> nanomaterials by laser irradiation in liquid, regulating irradiation time, laser energy density, NiCo<sub>2</sub>O<sub>4</sub> suspension concentration, etc. Fig.3 shows the SEM images of NiCo<sub>2</sub>O<sub>4</sub> suspensions after laser irradiation for 10 min at different energy densities. Compared with the raw NiCo<sub>2</sub>O<sub>4</sub> nanomaterials (Fig.3(a)), spheroidizing will be realized with the increase of laser energy density (Fig.3(b—f)). At the low energy density of 0.05 J·pulse<sup>-1</sup>·cm<sup>-2</sup>, only a few nanospheres appear, which attach on the NiCo<sub>2</sub>O<sub>4</sub> nanorods. This is because low laser energy is not enough to melt fully NiCo<sub>2</sub>O<sub>4</sub> nanomaterials, and achieve spheroidizing. As an increase in the laser energy density from 0.05 J·pulse<sup>-1</sup>·cm<sup>-2</sup> to 0.40 J·pulse<sup>-1</sup>·cm<sup>-2</sup>, NiCo<sub>2</sub>O<sub>4</sub> nanomaterials begin to melt, fuse and completely transform to the spherical nanoparticles (Fig.3(b—f)). The results reveal that there exists an energy density threshold, which can realize the complete spheroidizing of materials, because of the intrinsic characteristics of materials, such as melting point, boiling point, etc<sup>[13,14]</sup>. Furthermore, the obtained sample at the energy density of 0.30 J·pulse<sup>-1</sup>·cm<sup>-2</sup> has higher spheroidizing degree and superior dispersibility.

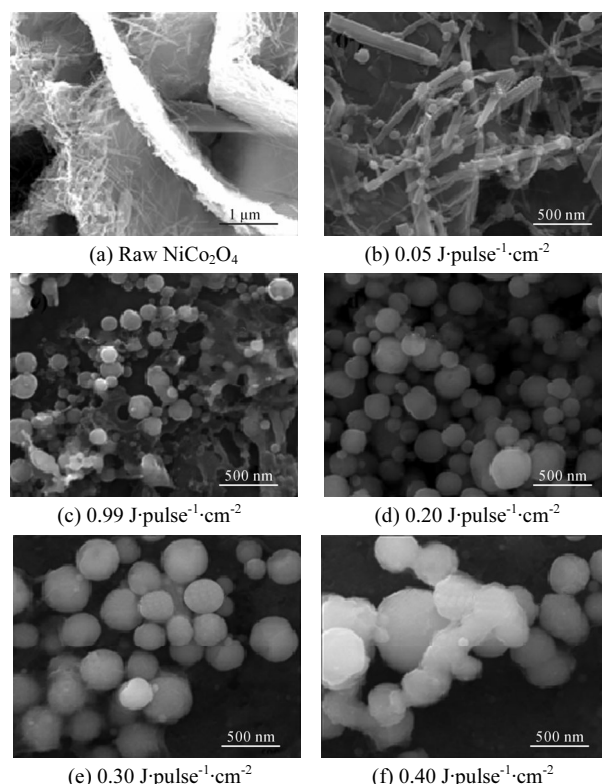


**Fig.3 SEM images of NiCo<sub>2</sub>O<sub>4</sub> suspensions after laser irradiation at different energy densities**

However, phase segregation will appear at high energy density, as shown in Fig.4. NiO or CoO phase presents in XRD patterns, with the increase of laser irradiation time, because of the solid redox of Co<sup>3+</sup>/Co<sup>2+</sup> and Ni<sup>3+</sup>/Ni<sup>2+</sup> existing in NiCo<sub>2</sub>O<sub>4</sub> nanomaterials, which can lead to redox reaction induced by laser. Therefore, during the

laser irradiation process, how to efficiently avoid or reduce the phase segregation of NiO or CoO is necessary.

Except laser energy density and irradiation time mentioned above,  $\text{NiCo}_2\text{O}_4$  suspension concentration is also crucial to the spheroidizing degree and superior dispersibility. Fig.5 shows SEM images of  $\text{NiCo}_2\text{O}_4$  suspensions with different concentrations after laser irradiation at  $0.30 \text{ J}\cdot\text{pulse}^{-1}\cdot\text{cm}^{-2}$  for 10 min. At the low suspension concentration of  $0.1 \text{ mg}\cdot\text{mL}^{-1}$  or  $0.2 \text{ mg}\cdot\text{mL}^{-1}$ , the obtained samples have a better size distribution and superior dispersibility (Fig.5(b,c)). As an increase in the suspension concentration from  $0.3 \text{ mg}\cdot\text{mL}^{-1}$  to  $0.5 \text{ mg}\cdot\text{mL}^{-1}$ , the spheroidizing degree and size distribution of the samples both reduce, with the dispersibility becoming worse (Fig.5 (d—f)).

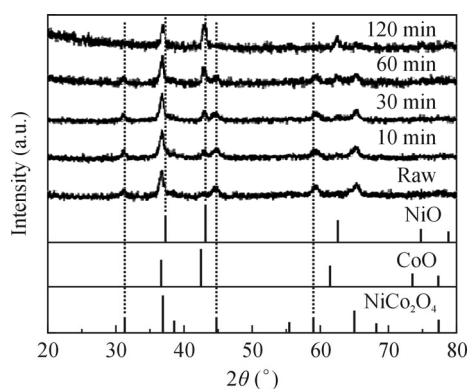


**Fig.4** XRD patterns of raw and laser-irradiation  $\text{NiCo}_2\text{O}_4$  nanomaterials

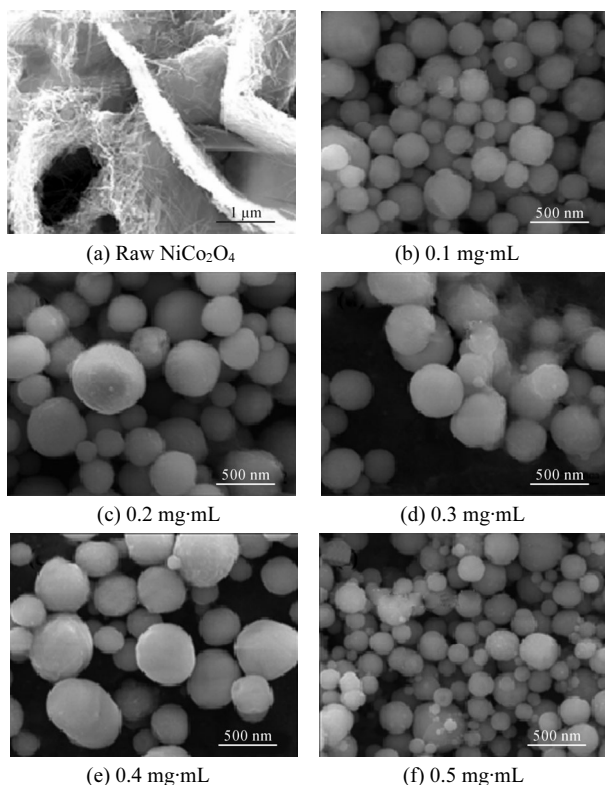


**Fig.5** SEM images of  $\text{NiCo}_2\text{O}_4$  suspensions with different concentrations after laser irradiation

The corresponding size distribution diagrams of  $\text{NiCo}_2\text{O}_4$  suspensions with different concentrations after laser irradiation are shown in Fig.6. With the suspension concentration increasing from  $0.1 \text{ mg}\cdot\text{mL}^{-1}$  to  $0.5 \text{ mg}\cdot\text{mL}^{-1}$ , the average size of the obtained samples firstly increases from 358 nm to 568 nm, and subsequently decreases to 310 nm (Fig.6(f) and Tab.1), because of the existing energy threshold, during the laser irradiation process. For low concentration  $\text{NiCo}_2\text{O}_4$  suspension, it can absorb enough energy to melt, fuse and transform to the spherical nanoparticles. However, with an increase in  $\text{NiCo}_2\text{O}_4$  suspension concentration, it will reduce the average laser energy density or even lower than the corresponding energy threshold, and not realize the spheroidizing or complete spheroidizing of  $\text{NiCo}_2\text{O}_4$  nanomaterials<sup>[14-16]</sup>. The results reveal that the obtained sample has higher spheroidizing degree and superior dispersibility with the maximal average size of 568 nm, as  $\text{NiCo}_2\text{O}_4$  suspension concentration of  $0.2 \text{ mg}\cdot\text{mL}^{-1}$ , laser energy density of  $0.30 \text{ J}\cdot\text{pulse}^{-1}\cdot\text{cm}^{-2}$  and irradiation time of 10 min.

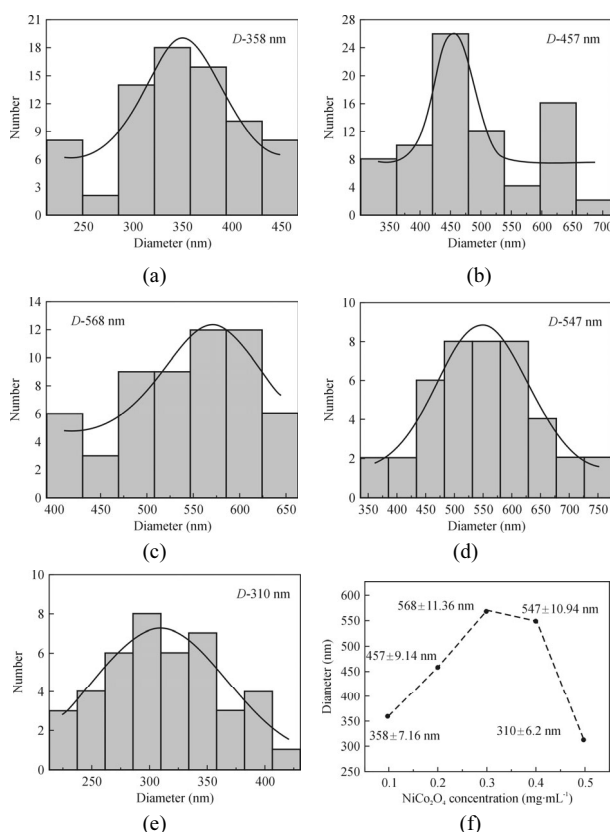


**Fig.6** Size distributions of  $\text{NiCo}_2\text{O}_4$  suspensions with different concentrations after laser irradiation

As the single-photon and multi-photon absorption of material associated with the light wavelength, we choose the 532 nm laser wavelength, which matches with the band edge absorption 560 nm of  $\text{NiCo}_2\text{O}_4$  nanomaterials. During laser irradiation process, the pulse laser energy

selectively only heats NiCo<sub>2</sub>O<sub>4</sub> nanoparticles instead of the liquid medium. At low laser energy density, it cannot make NiCo<sub>2</sub>O<sub>4</sub> nanomaterials melt, with simply heating and no other changes. With the laser energy density increasing to the melting point of NiCo<sub>2</sub>O<sub>4</sub> nanomaterials, it can absorb enough energy to melt, fuse and eventually transform to the spherical particles. Further increasing the laser energy density to or even exceeding the boiling point, it will lead to surface evaporation of spherical nanoparticles, and subsequently average size reduces. Therefore, the laser energy density is crucial to the spheroidizing of multi-oxides.

**Tab.1 Average sizes and error bars of NiCo<sub>2</sub>O<sub>4</sub> suspensions with different concentrations after laser irradiation**

Raw mass concentration (mg·mL <sup>-1</sup> )	Average size (nm)	Error bar (nm)
0.1	358	±7.16
0.2	457	±9.14
0.3	568	±11.36
0.4	547	±10.94
0.5	310	±6.20

The desired spheroidizing of NiCo<sub>2</sub>O<sub>4</sub> nanomaterials has been realized by laser irradiating NiCo<sub>2</sub>O<sub>4</sub> suspensions with different concentrations. The results reveal that the as-prepared samples are desired spheres with the maximal average size of 568 nm and the superior dispersity, which were obtained at the energy density of 0.30 J·pulse<sup>-1</sup>·cm<sup>-2</sup> and NiCo<sub>2</sub>O<sub>4</sub> suspension concentration of 0.2 mg·mL<sup>-1</sup>. However, the phase segregation, which was induced by large amounts of solid redox of Co<sup>3+</sup>/Co<sup>2+</sup> and Ni<sup>3+</sup>/Ni<sup>2+</sup>, also appears in the laser-irradiation process. The realization of spheroidized multi-oxides will promote the applications in electrochemical and catalysis fields.

## References

- [1] Zhu Y., Wu Z., Jing M., Hou H., Yang Y., Zhang Y., Yang X., Song W., Jia X. and Ji X., *J. Mater. Chem. A* **3**, 866 (2014).
- [2] Zhang C., Kuila T., Kim N. H., Lee S. H. and Lee J. H., *Carbon* **89**, 328 (2015).
- [3] Xu K., Li W., Liu Q., Li B., Liu X., An L., Chen Z., Zou R. and Hu J., *Journal of Materials Chemistry A* **2**, 4795 (2014).
- [4] Gao Z., Yang W., Wang J., Song N. and Li X., *Nano Energy* **13**, 306 (2015).
- [5] Wang Y., Cheng K., Cao D., Yang F., Yan P., Zhang W. and Wang G., *Fuel Cells* **15**, 298 (2015).
- [6] Cui B., Lin H., Li J.-B., Li X., Yang J. and Tao J., *Advanced Functional Materials* **18**, 1440 (2008).
- [7] Wang Q., Liu B., Wang X., Ran S., Wang L., Chen D. and Shen G., *Journal of Materials Chemistry* **22**, 21647 (2012).
- [8] Zhang G. and Lou X. W., *Advanced Materials* **25**, 976 (2013).
- [9] Mondal A. K., Su D., Chen S., Kretschmer K., Xie X., Ahn H. J. and Wang G., *Chemphyschem* **16**, 169 (2015).
- [10] Jokar E., zad A. I. and Shahrokhian S., *Journal of Solid State Electrochemistry* **19**, 269 (2014).
- [11] Li X., Jiang L., Zhou C., Liu J. and Zeng H., *NPG Asia Materials* **7**, e165 (2015).
- [12] Cui B., Lin H., Liu Y.-z., Li J.-b., Sun P., Zhao X.-c. and Liu C.-j., *The Journal of Physical Chemistry C* **113**, 14083 (2009).
- [13] Wang H., Pyatenko A., Kawaguchi K., Li X., Swiatkowska-Warkocka Z. and Koshizaki N., *Angewandte Chemie International Edition* **49**, 6361 (2010).
- [14] Wang H., Koshizaki N., Li L., Jia L., Kawaguchi K., Li X., Pyatenko A., Swiatkowska-Warkocka Z., Bando Y. and Golberg D., *Advanced Materials* **23**, 1865 (2011).
- [15] Pyatenko A., Wang H. and Koshizaki N., *The Journal of Physical Chemistry C* **118**, 4495 (2014).
- [16] Pyatenko A., Wang H., Koshizaki N. and Tsuji T., *Laser & Photonics Reviews* **7**, 596 (2013).